Available online at www.sciencedirect.com
SCIENCE DIRECT®
Journal of Power Sources 157 (2006) 765–774
JOURNAL OF POWER SOURCES
www.elsevier.com/locate/jpowsour

Process analysis of a molten carbonate fuel cell power plant fed with a biomass syngas

C. Tomasi [a], M. Baratieri [a], B. Bosio [b,*], E. Arato [b], P. Baggio [a]

[a] *DICA, University of Trent, Italy*
[b] *DIAM, University of Genoa, Italy*

Received 1 October 2005; accepted 9 December 2005
Available online 24 January 2006

Abstract

The coupling of renewable energy sources and innovative power generation technologies is of topical interest to meet demands for increased power generation and cleaner environmental performance. Accordingly, biomass is receiving considerable attention as a partial substitute for fossil fuels, as it is more environmentally friendly and provides a profitable way of disposing of waste. In addition, fuel cells are perceived as most promising electrical power generation systems. Today, many plants combining these two concepts are under study; they differ in terms of biomass type and/or power plant configuration. Even if the general feasibility of such applications has been demonstrated, there are still many associated problems to be resolved. This study examines a plant configuration based on a molten carbonate fuel cell (MCFC) and a recirculated fluidized-bed reactor which has been applied to the thermal conversion of many types of biomass. Process analysis is conducted by simulating the entire plant using a commercial code. In particular, an energy assessment is studied by taking account of the energy requirements of auxiliary equipment and the possibility of utilizing the exhaust gases for cogeneration.

Keywords: Molten carbonate fuel cell; Biomass; Energy analysis; Simulation; Fluidized-bed gasifier; Power plant

1. Introduction

In recent years, there has been a notable increase in the number of published studies on the combined use of fuel cells and biomass. Nevertheless, only a few practical applications have been made internationally. At present, researchers are focusing on the prospects of this new technology as a means to meet increasingly strict environmental constraints, provide good process efficiency, and make use of new fuel sources. At the same time, they are also investigating improvements in plant and process solutions.

In the present study, a plant configuration is proposed and is based on a main power generator consisting of a molten carbonate fuel cell (MCFC) stack and a recirculated fluidized-bed reactor which has been applied to the thermal conversion of many types of biomass, e.g., pine wood sawdust, poplar wood sawdust, bagasse, cotton stalks, almond shells, residue from olive pressing. Process analysis is carried out by simulating the entire plant using a *Simulink* model, which is made up of a series of objects that represent a set of functions written in *Matlab*®. The plant operation is optimized in terms of energy management, which also includes cogeneration. An exergy analysis has been performed and the results show good system performance.

2. The reference plant

The layout of the reference plant (Fig. 1) is characterized by complete integration of the synthesis gas (syngas) production and electrochemical sections. The former is represented by a recirculated fluidized-bed gasifier, which consists of a gasification reactor heated by a furnace. For the thermochemical conversion process, several types of biomass are considered as feedstock. The resulting syngas is piped through a clean-up section to the MCFC stack and represents the 'anodic flow'. The gasification process is endothermic and the heat necessary to sustain the reactions is supplied by a coupled burner in which the solid carbon-based product (char) is oxidized with the anodic exhaust gas and, if necessary, auxiliary fuel. All the gas produced

* Corresponding author. Tel.: +39 010 353 6505; fax: +39 010 353 2589.
E-mail address: bosio@diam.unige.it (B. Bosio).

0378-7753/$ – see front matter © 2005 Elsevier B.V. All rights reserved.
doi:10.1016/j.jpowsour.2005.12.038

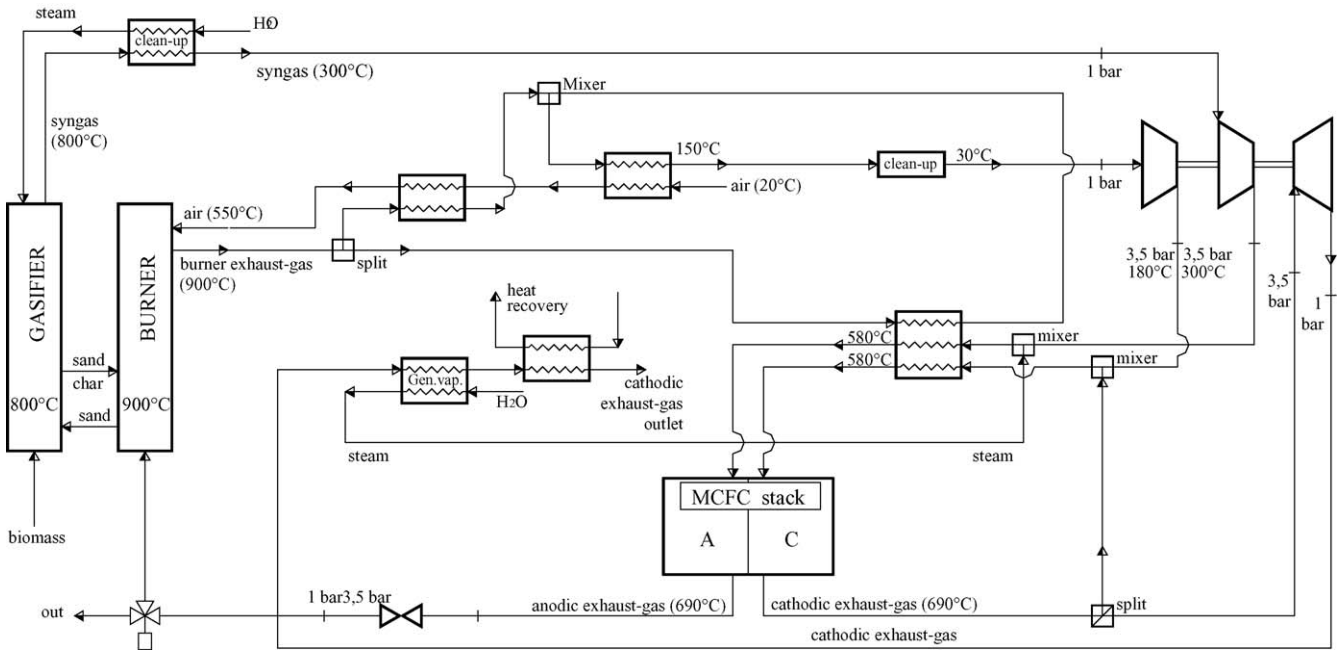

Fig. 1. Reference plant layout.

by the burner is subjected to a clean-up process and represents the 'cathodic flow' for the MCFC stack.

The optimum operating condition of the MCFC stack is at a pressure of about 3.5 bar. Since the gasification process is conducted at atmospheric pressure to avoid complex design choices, the production and the electrochemical sections work at different pressures. The anodic and cathodic flows are compressed prior to entry into the MCFC stack, while some power is recovered by expanding the cathodic exhaust gas in the turbine. The same energy recovery is not considered for the smaller anodic flow because of the risks related to the presence of hydrogen, so a simple throttling valve is installed in place of the turbine.

The anodic flow feeding the stack, and consequently the amount of treated biomass, depends on the power demand, given that a fuel utilization factor of 75% is imposed in the cells. The concentration of CO_2 and O_2 entering the cathode as well as the stack operating temperature are controlled by means of the recirculation factor and the flow rate of the fresh air stream. In order to ensure combined heat and power (CHP) production, a thermal energy recovery system has been included for the cathodic exhaust gas outlet stream and the syngas clean-up module.

3. Biomass thermal conversion system

The adopted system configuration consists of a recirculated fluidized-bed reactor in which pyrolysis or gasification with steam is conducted out (Fig. 2). As mentioned above, this system requires an external energy source, namely, a burner fed with the residual char and auxiliary fuel. In some plants, a syngas recirculation system is incorporated in the burner in order to assure optimum chemical conversions and high process temperatures [1]. In a similar way, the anodic exhaust gas is used as a fuel in the combustion chamber. Recirculation of the fluidized-bed sand between the two modules allows heat exchange and sustains the chemical reaction.

The burner temperature, fixed at 900 °C, should be monitored with appropriate sensors in order to assess the correct amount of auxiliary fuel that is required to keep the temperature constant. The system should include an outlet valve to discharge the excess gas in case the quantity of char and anodic exhaust gas causes the temperature to rise above the desirable value. Using this configuration, it is advisable to grind the biomass into small chips in order to maximize the specific contact surface between the solid and gas phases.

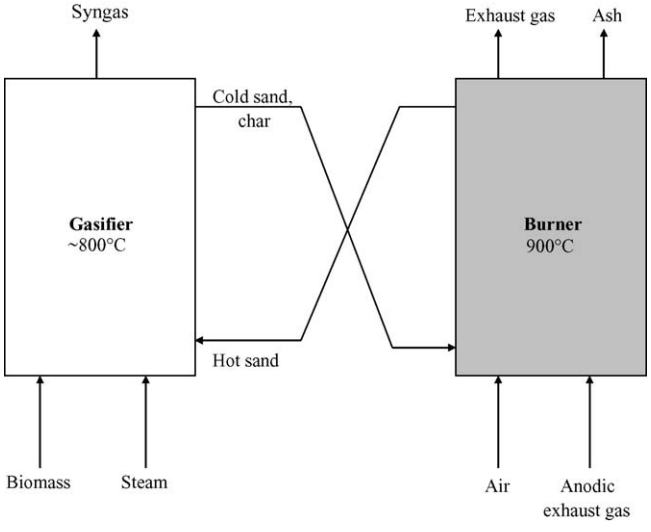

Fig. 2. Biomass thermal conversion plant outline: adopted configuration.

The output products of the gasifier are syngas, solid phase (char), and liquid phase (tar).

The char is a complex agglomerate that consists of solid carbon, ash, sulfurous compounds, and volatile hydrocarbons. The ash and sulfur fractions in the char produced by thermal biomass conversion are small, and carbon predominates. The first step in the deposition of solid carbon is represented by the agglomeration of molecules with atomic masses between 500 and 2000 u.m.a.; the growth in particle dimensions over time is due to coagulation phenomena and the superficial deposition of acetylene. The deposition of residual solid carbon is characterized by the fixed carbon, which is calculated with the gasification model developed in this work.

The ash production from the conversion process has been estimated using literature data. It appears reasonable to assume that this inert fraction is not involved in the process reactions. For evaluation of the enthalpy, an average ash composition with 50% CaO and 50% SiO_2 has been considered [2].

The tar is a liquid product that consists of organic molecules and oils with high molecular weight. The great viscosity and acidity that characterize this product make its removal difficult. For this reason, it is desirable to promote tar-cracking processes in the gasification chamber (i.e., to convert the tar into small-chain molecules) by means of a proper catalyst such as sintered dolomite mixed with sand in the reactor bed.

Various approaches can be used to calculate the equilibrium composition of the syngas. For this purpose, a code written in Matlab language has been formulated in order to use the available equilibrium solver implemented in *Cantera*. The latter is a collection of object-oriented software tools for problems involving chemical kinetics, thermodynamics, and transport processes [3]. The algorithm implemented in *Cantera* is a version of the Villars-Cruise-Smith (VCS) algorithm, which finds the composition that minimizes the total Gibbs free energy of an ideal mixture [4]. The NASA database has been used for the thermodynamic properties of the species utilized in the model [5].

In order to estimate the yield of gaseous products and solid carbon, a multiphase formulation of the model has been used. The default ideal gas mixture that represents one of the two considered phases consists of 57 different gaseous species. The implemented solver finds the effluent composition that minimizes the Gibbs free energy and takes into account more than 300 reactions. Only a few gaseous species are present in the syngas in significant percentages, namely: hydrogen, steam, methane, carbon monoxide, carbon dioxide, nitrogen, and oxygen.

The presence of small amount of methane in the gaseous product suggests that it is possible to avoid a reforming stage in order to simplify the plant management. The concentration of nitrogen is negligible, since there is no additional air and its presence in the biomass is about 0.2 wt.%.

The calculated yield of solid carbon can be related to the actual charcoal residue of the thermal conversion process. Variation of the amount of solid with process temperature and pressure, evaluated by the implemented equilibrium model, can be confirmed by the Boudouard heterogeneous equilibrium reaction.

4. Clean-up treatment

The presence of by-products in the syngas makes it necessary to clean-up the gaseous flow prior to its use by the electrochemical section. There are different syngas clean-up processes, depending on the feedstock, on the adopted thermal conversion process and on the stack demand. Molten carbonate fuel cells (and the other cells operating at high temperatures) have a greater tolerance of impurities than low-temperature cells. Nevertheless, some undesirable species tend to accumulate inside the cells and cause a decrease in performance and reliability. For example, particulate matter and tar tend to settle on the cell surface so as to obstruct the section available for gas flow and reduce the contact surface between the gas and the catalyst.

Alkali metals and halogenous and nitrogenous compounds may react with the electrolyte and cause its loss, while sulfur-containing compounds have harmful effects on the catalyst. The tolerance limits of gas impurities for MCFC stacks are presented in Table 1. Particulate matter can be effectively removed from the syngas flow by means of cyclones and other filtration systems (e.g., electrostatic precipitators, ceramic and bag filters) that may have removal efficiencies up to 99.8%. Alkali metals condense at temperatures lower than 500 °C and can also be removed with the particulate matter. The tar fraction is usually removed by catalytic cracking processes, or by means of filtration and scrubbing treatment. The latter is particularly effective in removing halogenous, nitrogenous and sulfur compounds.

Given the cell tolerances and available treatment options, two different configurations have been selected for the anodic and cathodic clean-up processes. The most reliable methods are based on significant gas cooling and, as a consequence, cause serious thermal energy losses. In both cases, the plant balance has been optimized in order to maximize the production of combined heat and power.

Table 1
Tolerance limits of impurities for MCFC stacks [12]

Pollutant	Tolerance limits (ppm)	References
Particulate matter	10	[6–9]
Tar	2000 (C_6H_6)	[8]
Halogenous (HCl)	<0.1	[6–8]
Sulfur (H_2S)	0.1	[6–9]
COS, CS_2, mercaptan	1	[10]
Nitrogenous (NH_3)	0.1	[7–10]
Hydrocarbons (C_2–C_6)	<12 vol.% (saturated) <0.2 vol.% (olefin) <0.5 vol.% (cyclic) <0.5 vol.% (aromatic)	[6,7]
Heavy metals	As < 0.1 ppm Zn < 15 ppm Cd < 30 ppm Hg < 35 ppm Pb < 1 ppm	[8]
Alkali metals	1–10 ppm	[6,11]

4.1. Anodic clean-up

The entire clean-up treatment is characterized by a pressure of 1 bar, since the thermal conversion process is conducted at atmospheric pressure. The syngas pressure is successively increased to the cell operative value, equal to 3.5 bar, by means of a compressor placed before the electrochemical section. The chosen system, developed by Coppola et al. [12], consists of the following treatment units.

- A tar cracker for thermal conversion of heavy hydrocarbons, operating at a process temperature of 1200 °C.
- A first heat-exchanger, which decreases the gas temperature.
- A first cyclone for removal of particulate matter with diameters greater than 5 μm.
- A zinc oxide reactor, which allows the adsorption of sulfur compounds, and a sodium carbonate reactor for halogenous compounds.
- A second heat-exchanger, which further lowers the gas temperature.
- A second cyclone followed by an electrostatic precipitator and a ceramic filter in order to remove particulate matter with smaller diameters and the solid fraction coming from the previous unit.

Since the burner temperature is fixed at 900 °C, a temperature of 1200 °C is not easily reachable in the tar cracker. Therefore, in this study, sintered dolomite has been mixed with the sand in the reactor bed to promote cracking in the gasifier. The technique has a maximum efficiency at process temperatures between 750 and 900 °C and this makes it possible to eliminate the cracking unit [13].

The anodic clean-up process parameters are summarized in Table 2.

The adopted plant scheme is represented in Fig. 3. After the ceramic filter, the syngas is piped to the electrochemical section. In the anodic clean-up plant, the recovered heat from the two coolers may be used to produce superheated steam to be used, if necessary, as an oxidizing agent in the gasification stage.

Table 2
Process parameters for anodic gas clean-up treatment simulation [12] (η = efficiency)

Plant unit	Process parameter
Cyclone 1	$T = 400\,^{\circ}C$; $\eta = 90\%$
Adsorber	$T = 400\,^{\circ}C$; $F_{Na2CO3} = 0.01\ kmol\ h^{-1}$; $F_{ZnO} = 0.01\ kmol\ h^{-1}$
Cyclone 2	$T \sim 300\,^{\circ}C$; $\eta = 90\%$
Electrostatic precipitator	$T \sim 300\,^{\circ}C$; $\eta = 99\%$
Ceramic filter	$T \sim 300\,^{\circ}C$; $\Delta P = 25$ mbar

4.2. Cathodic clean-up

The cathodic gas consists of the combustion products leaving the burner. Here the char fraction produced in the gasifier, the anodic exhaust gas, and, if necessary, an auxiliary fuel (additional biomass) is burned.

The usual gas purification outline for a biomass plant has been adopted here, providing for a cyclone, a bag filter and a scrubber. The incoming gas flowing to the clean-up module is cooled in a counter-current heat-exchanger at a temperature of about 150 °C, by means of the pre-heating of the air piped to the burner, and the anodic and cathodic gases, whose temperatures before entering the MCFC stack are fixed at 580 °C. Then, it passes through the cyclone, which is capable of removing particulate matter of a diameter greater than approximately 5 μm, and through the bag filter, which has a high removal efficiency for a wide range of granulometries [14]. The gas is then treated with a scrubber, which reduces its temperature to less than 100 °C. This purification process favours steam condensation and the removal of sulfur and halogenous compounds, so increasing cell reliability. The outlet stream, which has a temperature of 30 °C (adiabatic saturation temperature), is compressed to the operative stack pressure. Existing scrubbing technologies do not allow for the recovery of the latent water heat and there by

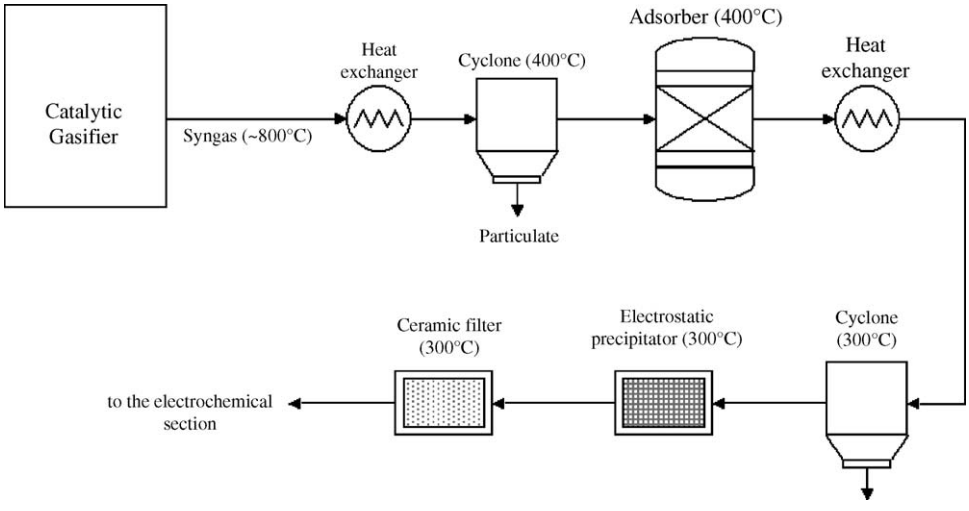

Fig. 3. Anodic clean-up plant scheme.

Table 3
Process parameters for simulation of the cathodic gas clean-up treatment [14].

Plant unit	Process parameter
Cyclone	$T = 130\,^{\circ}C$; $\eta = 90\%$
Bag filter	$T = 130\,^{\circ}C$; $\Delta P = 10$–25 mbar; $\eta > 99\%$
Scrubber	$T_{in} = 30\,^{\circ}C$; $T_{out} = 130\,^{\circ}C$; $\Delta P = 6$–25 mbar

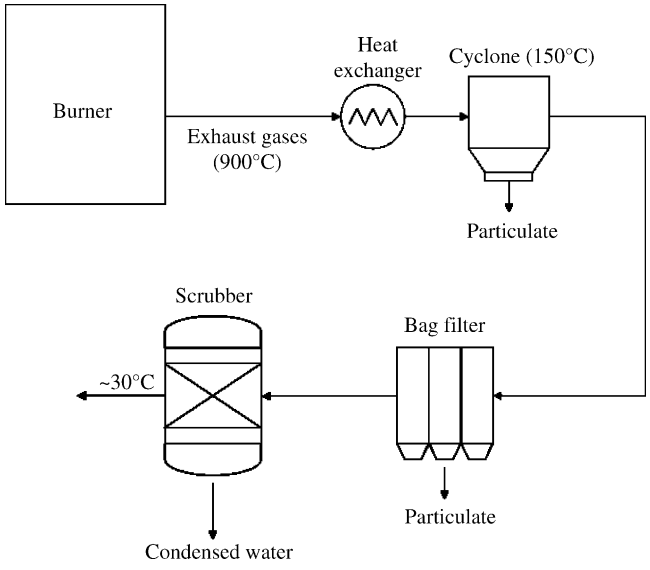

Fig. 4. Cathodic clean-up plant scheme.

cause a significant energy loss for the whole system. The data used for this clean-up section are reported in Table 3 and the plant scheme adopted is represented in Fig. 4.

5. Fuel cell system

Fuel cells represent one of the most promising technologies to produce clean energy. Recently, the interest in these power generation devices has grown considerably and it is believed that they will play a fundamental role in future distributed energy supplies.

Molten carbonate fuel cells have been selected for this study because of their high energy output, lower sensitivity to contaminants, suitability to combined heat and power generation (due to high operating temperature), and the developed state-of-the-art. As a practical example, the technology developed by Ansaldo Fuel Cells (Genova, Italy) has been chosen.

The usefulness of reference Ansaldo MCFC plant configurations for the proposed application with biomass syngas has been verified in previous work from the standpoint of both energy and environmental issues [15,16]. In this study, a better integration between the biomass treatment section and the MCFC is obtained. Moreover, the previous MCFC systems were characterised by external reforming, but the presence of a methane reforming stage is not suitable when methane-poor syngas is used [17].

In this paper, external reforming is not considered and it has been assumed that the methane in the MCFC is inert. The simulated MCFC unit supplies about 250 kW and consists of two

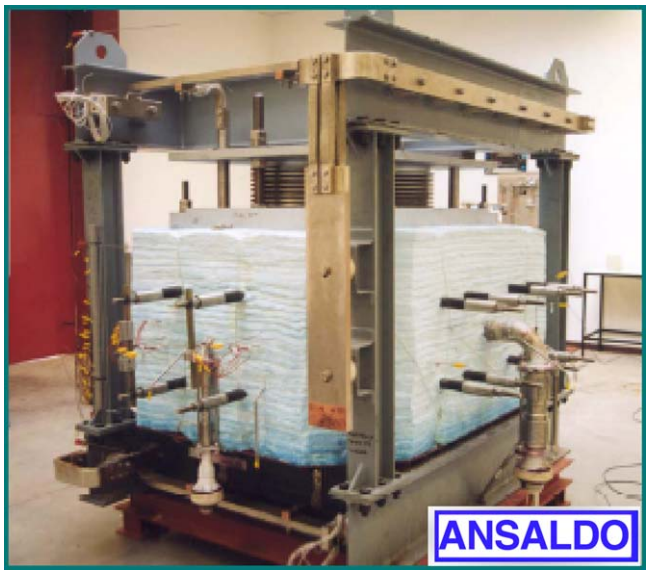

Fig. 5. Molten carbonate fuel cell stack.

stacks of 150 cells, each with a surface area of 0.711 m^2 Fig. 5. The developed model is zero-dimensional and a constant electric resistance value of 1.67 Ωm^2 has been assumed for each cell.

The electrochemical reaction rate is fixed by the 75% fuel utilization, controlled by proper biomass feeding. The water–gas shift reaction occurring at the anode is assumed to be at the thermodynamic equilibrium and the resulting gas conditions are calculated using *Cantera* (see Section 3).

Additional steam is fed upstream of the stacks to preclude the Boudouard reaction, as carbon deposition is dangerous for the system because it obstructs the gas flow and reduces stack efficiency.

Before entering the stack, the temperature of the anodic and cathodic inlet streams are fixed at 580 °C, since lower temperatures prevent an adequate ionic exchange. Moreover, the temperature in the cell must not exceed 700 °C in order to avoid corrosion and loss of electrolyte. This limit is assumed by feeding the correct amount of fresh air to the burner (the recirculation factor ranges are between 30 and 40%). By means of the same operating parameter management, the concentrations of carbon dioxide and oxygen entering the cathode are controlled. A pressure loss of 20 mbar in the MCFC stack has been taken into account.

6. Results and discussion

6.1. Mass balance and product characterization

Several types of biomass have been used as feedstocks, namely, pine wood sawdust, poplar wood sawdust, bagasse (residue of sugar cane pressing and grinding), cotton stalks, almond shells, residue of olive pressing. They all consist of industrial, agricultural and forest waste matter readily available on the market.

To optimize the biomass thermal conversion process, the proper steam to carbon ratio (S:C) has been calculated (S:C

Table 4
Ultimate analysis and calculated conversion temperature of feedstocks

	Bagasse [18]	Pine sawdust [18]	Poplar sawdust [18]	Cotton stalks [18]	Almond shells [19]	Olive wastes [19]
Moisture (wt.%)	7.1	9.4	10.0	7.9	11.50	13.03
Ash (wt.%)	0.9	0.9	3.9	4.5	2.92	3.57
C (wt.%)	46.0	45.2	43.1	42.8	40.91	41.70
H (wt.%)	5.4	5.4	5.1	5.3	5.13	5.17
O (wt.%)	40.4	39.0	37.7	38.5	38.60	35.20
N (wt.%)	0.2	0.1	0.2	1.0	0.94	1.33
Conversion temperature (°C)	795	798	781	774	830	806

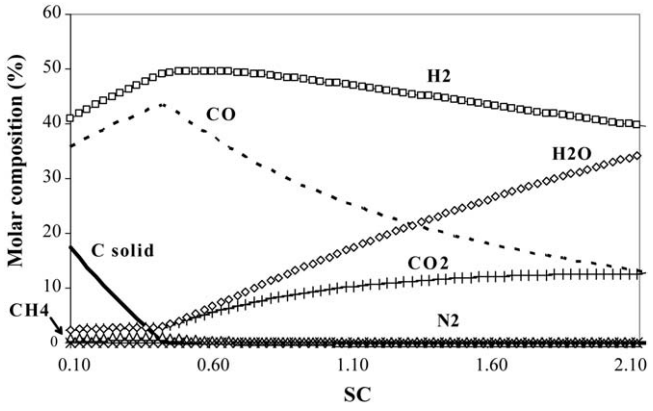

Fig. 6. Gaseous and solid products for thermal conversion of bagasse: molar composition as function of steam to carbon ratio (S:C) (pressure = 1 bar; temperature = 795 °C).

is defined as the ratio of the amount of inlet steam to the carbon fraction present in the feedstock).

The solid fraction as a function of S:C for the bagasse is shown in Fig. 6. As expected, the production of solid carbon decreases with increasing S:C, since, as the oxidant power rises, the residual solid matter is subjected to a gasification process.

The equilibrium simulations show that the proper S:C value is reached using only the water fraction found in the biomass, so that the combustion of the solid carbon produced allows the process to be auto-thermal. In fact, if the solid carbon fraction is insufficient, an auxiliary fuel must be burned in the furnace. This causes a decline in global efficiency despite of the increased syngas-production efficiency.

The gasifier temperature, optimized in order to produce the right fraction of solid carbon, is different for each feedstock, as shown in Table 4, in which the ultimate analysis of the feeding materials is also included.

The molar fraction composition of the syngas calculated for each feedstock is given in Table 5. As discussed, no oxidizing agent has been used in the cases studied, so that the biomass is pyrolyzed. Similarly, the characterization of the burner exhaust gas is presented in Table 6.

The synthesis gas and the burner exhaust gas represent the anodic and cathodic streams, respectively. The total and the gaseous species molar flows entering and leaving the MCFCs are reported in Table 7 for the case of the pine wood sawdust

Table 5
Syngas characterization in molar percent composition

	Bagasse	Pine sawdust	Poplar sawdust	Cotton stalks	Almond shells	Olive wastes
H_2	49.49	50.19	49.46	49.35	49.44	50.85
H_2O	2.99	2.88	3.55	4.33	1.93	2.57
CO	43.33	43.00	42.02	39.77	45.48	42.38
CO_2	2.88	2.69	3.50	4.31	1.74	2.28
CH_4	1.18	1.18	1.34	1.58	0.85	1.12
N_2	0.13	0.06	0.13	0.66	0.56	0.80
O_2	0.00	0.00	0.00	0.00	0.00	0.00

Table 6
Cathodic gas characterisation in molar percent composition

	Bagasse	Pine sawdust	Poplar sawdust	Cotton stalks	Almond shells	Olive wastes
H_2	0.00	0.00	0.00	0.00	0.00	0.00
H_2O	18.40	18.92	18.82	18.23	20.94	20.00
CO	0.00	0.00	0.00	0.00	0.00	0.00
CO_2	11.27	11.34	11.32	11.26	11.55	11.48
CH_4	0.00	0.00	0.00	0.00	0.00	0.00
N_2	58.53	57.94	58.04	58.67	55.75	56.75
O_2	11.80	11.80	11.82	11.82	11.76	11.77

Table 7
Temperature, total and gaseous species mass molar flows related to inlet and outlet stack stream (pine sawdust simulation)

Pine sawdust	Anode		Cathode	
	Inlet stream	Outlet stream	Inlet stream	Outlet stream
Temperature (°C)	580.0	692.8	580.0	691.4
Mass flow (kmol h^{-1})	20.42	26.06	130.51	122.03
H_2 (kmol h^{-1})	4.07	2.47	0.00	0.00
H_2O (kmol h^{-1})	12.55	14.68	0.00	0.00
CO (kmol h^{-1})	3.48	0.81	0.00	0.00
CO_2 (kmol h^{-1})	0.22	8.00	16.16	10.51
CH_4 (kmol h^{-1})	0.09	0.09	0.00	0.00
N_2 (kmol h^{-1})	0.01	0.01	96.12	96.12
O_2 (kmol h^{-1})	0.00	0.00	18.23	15.40

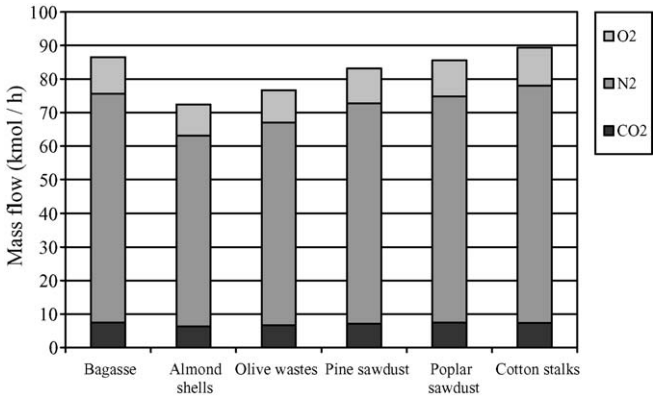

Fig. 7. Characterization of the plant exhaust emissions.

Table 8
Plant exhaust emission temperature and mass flows

	Mass flow (kmol h^{-1})	Temperature (°C)
Bagasse	86.57	261.4
Almond shells	72.37	220.4
Olive wastes	76.66	238.7
Pine sawdust	83.17	254.3
Poplar sawdust	85.63	259.7
Cotton stalks	89.39	271.7

conversion. Also shown are the stream temperatures as required by the operating constraints.

The mass flow, the temperature and the characterization of the plant exhaust emissions are presented in Table 8 and in Fig. 7, for each type of fuel.

Finally, Fig. 8 shows all the calculated flows using the mass balance resulting from the simulation of the whole process for the reference case of the pine wood sawdust conversion. Because of the great amount of water condensed in the scrubber of the cathodic clean-up system, it would be reasonable to recover a fraction of it, through a purification treatment, in order to pump it to the mixer module on the anodic stream. The heat and mass fluxes have been characterized for each feedstock in order to assess the global efficiency. Since the plant configuration permits both heat and electrical power generation, the thermal and electrical efficiencies have been evaluated separately. Moreover, an exergy balance has been performed to quantify the efficiency with a single parameter.

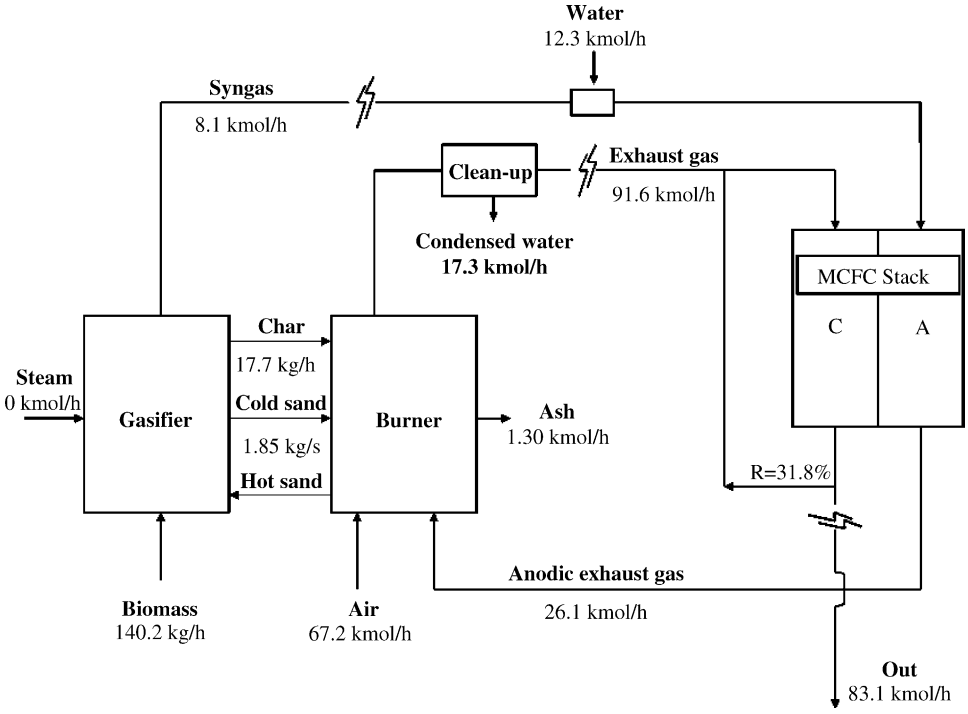

Fig. 8. System mass balance for simulation conducted with pine sawdust.

Table 9
Current density and cell voltage calculated for MCFC unit for each feedstock

Biomass	Current density (A m^{-2})	Cell voltage (V)
Bagasse	1430	0.819
Pine sawdust	1422	0.824
Poplar sawdust	1449	0.809
Cotton stalks	1470	0.797
Almond shells	1381	0.848
Olive wastes	1403	0.835

6.2. Energy balance and process efficiency

The energy balance management has been optimized for the whole process in order to assess the total efficiency. The used and recovered energy have been calculated in terms of electricity, heat and mechanical energy for the thermal conversion and electrochemical sections. The electrical energy produced has been calculated from the sum of the power generated by the stack and the turbine minus the auxiliary consumptions. The MCFC stacks, as discussed above, have been simulated with a simplified model and supply a nominal electrical power of 250 kW according to Table 9.

A 99% efficiency has been assumed for the alternator; the calculated power is simply the exhaust gas expansion work from which the syngas and cathodic stream compression work has been subtracted. Although the compression and expansion isentropic efficiency has been fixed at 85%, values between 91 and 95% can be reached, even for sizes greater than 10 kW [20].

The thermal energy consists of the fraction recovered from the anodic and cathodic streams. In particular, since no steam is piped to the gasifier, the entire contribution before the anodic clean-up is recovered for heat generation. Similarly, it is possible to contemplate the same recovery process at the cathodic exhaust gas outlet. The abovementioned cooling process is also beneficial for the next compression process, as the related work is a function of the specific volume of the gas and, so, of its temperature. Heat-exchanger efficiency has been assumed to be 75% for the processes involving only gas phases, and 85% in the case of a liquid–gas heat-exchange process. In the simulations the clean-up system power consumptions have not been considered, but can be estimated to be lower than 10 kW [14].

The plant efficiency has only been calculated for the generation of electrical power in the case of combined heat and power production. The latent heat has not been taken into account in the recovery of the available thermal energy from the exhaust gases since the lower heating value has been considered for the feedstock. The average value of the electrical energy efficiency is significantly greater than the corresponding parameter related to gasification plants, where the syngas is usually fed to conventional otto and diesel engines. In these cases, the electrical efficiency is approximately 20–21%. A biomass amount of 460–550 g (respectively, for almond shells and cotton stalks) has been quantified to produce 1 kW h of electric energy.

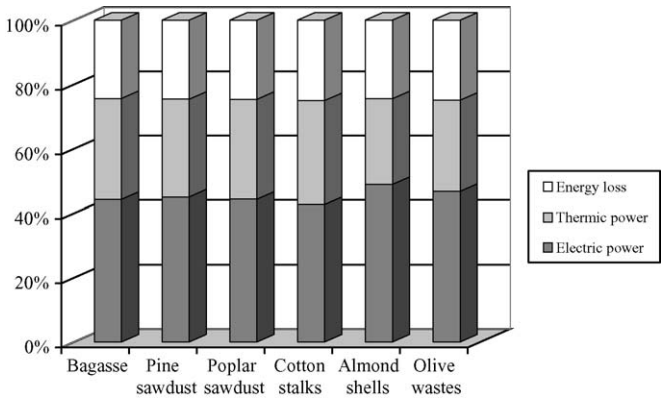

Fig. 9. Electrical and thermal energy production percentage, with respect to biomass lower heating value.

The global efficiencies obtained from the sum of the electrical and thermal generated power versus the lower heating value are given in Table 10, while a histogram showing the percentage of produced energy is presented in Fig. 9. The results obtained in the different cases studied are very similar due to the analogous ultimate analysis.

A major fraction of the energy loss is due to the difficulty of recovering the thermal energy wasted by the scrubber (inlet and outlet temperatures of about 150 and 30 °C, respectively). A minor energy loss arises from the enthalpy of the ash that exits the thermal conversion section and from the unrecovered heat from the exhaust in the temperature range 20–30 °C. As electrical and thermal powers do not have the same exergy value, the process exergy efficiency has been evaluated as the ratio between exergy entering the plant and exergy supplied in the form of electrical and thermal energy. Electrical and mechanical energy can be considered as pure exergy. By contrast, the energy given off in a combustion process, i.e., the heating value, cannot be totally exploited, and the corresponding exergy can be evaluated using the following expression:

$$E_{\text{biomass}} = \int_{T_{\text{adiabatic}}}^{T_{\text{exhaust}}} \left(1 - \frac{T_0}{T}\right) c_p^{\text{exhaust}} \mathrm{d}T \quad (1)$$

Table 10
Electrical and thermal energy plant efficiencies

Biomass	Lower heating value (kW^{t})	Electrical power (kW^{e})	Thermal power (kW^{t})	Electrical efficiency (%)	Electrical and thermal efficiency (%)
Bagasse	656.1	290.3	206.0	44.2	75.6
Pine sawdust	638.7	287.4	194.0	45.0	75.4
Poplar sawdust	653.2	289.2	203.1	44.3	75.4
Cotton stalks	684.4	292.0	221.1	42.7	75.0
Almond shells	572.0	279.6	152.5	48.9	75.5
Olive wastes	604.2	282.5	171.1	46.8	75.1

Table 11
Exergy efficiency calculation of plant, for each type of biomass

	Bagasse	Pine sawdust	Poplar sawdust	Cotton stalks	Almond shells	Olive wastes
Exergy recovered in the clean-up module (kW)	22.8	23.0	23.1	22.7	22.7	22.8
Exergy recovered by the plant exhaust (kW)	48.2	44.0	47.1	53.7	23.2	36.0
Biomass exergy (kW) (1st method)	457.3	445.2	453.4	474.3	403.0	421.5
Biomass exergy (kW) (2nd method)	470.9	458.4	468.8	491.2	410.5	433.6
Exergy plant efficiency (kW) (1st method)	79.0	79.6	79.3	77.7	80.8	81.0
Exergy plant efficiency (kW) (2nd method)	76.7	77.3	76.7	75.0	79.3	78.7

where T_0 is the environmental temperature; $T_{\text{adiabatic}}$ the adiabatic combustion temperature; T_{exhaust} the exhaust gas temperature; and c_p is the specific heating value at constant pressure, as a function of temperature.

The adiabatic combustion temperature can be calculated as follows:

$$T_{\text{adiabatic}} = T_0 + \frac{\text{LHV} + \dot{m}_{\text{air}} \int_{T_0}^{T_{\text{air}}} c_p^{\text{air}} \mathrm{d}t}{\dot{m}_{\text{exhaust}} \int_{T_0}^{T_{\text{adiabatic}}} c_p^{\text{exhaust}} \mathrm{d}t / (T_{\text{adiabatic}} - T_0)} \quad (2)$$

where LHV is the lower heating value of the fuel; $\dot{m}$ refers to the gas mass flow; and T_{air} is the initial temperature value of the oxidant (air).

As the adiabatic combustion temperature is in the denominator of the equation, the calculation has to be carried out iteratively, to obtain the solution of Eq. (1).

The exergy efficiency of the whole process can be obtained as follows:

$$\eta_{\text{ex}} = \frac{1}{\dot{m}_{\text{biomass}} E_{\text{biomass}}} \left(P_{\text{el}} + \int_{T_{\text{in}}}^{T_{\text{out}}} (1 - T_0/T) \dot{m}_{\text{syngas}} c_p^{\text{syngas}} \mathrm{d}T + \int_{T_{\text{exhaust}}}^{T_{\text{min}}} (1 - T_0/T) \dot{m}_{\text{exhaust}} c_p^{\text{exhaust}} \mathrm{d}T \right) \quad (3)$$

where P_{el} is the electrical power supplied; T_{in} and T_{out} the syngas inlet and outlet temperatures of the clean-up module, respectively; and T_{exhaust} and T_{min} are the plant exhaust temperature, and the minimum exploitable exhaust temperature, respectively.

As a verification, the efficiency evaluation has been repeated using a second method, in which the Gibbs free energy produced in a complete combustion process has been used as the biomass exergy value. The method is analogous to evaluation of fuel cell efficiency, where the maximum available energy is the free energy of the supplied fuel.

It is difficult to find biomass free energy values in the literature, while the heating value is usually known. Therefore, it has been supposed that the ratio between the well-known Gibbs free energy and heating value of cellulose is similar to that of biomass. The biomass free energy has been consequently obtained with the expression:

$$\Delta G_{\text{biomass}} = \text{LHV} \left(\frac{\Delta G^0_{\text{cellulose}}}{\Delta H^0_{\text{cellulose}}} \right) \quad (4)$$

where LHV is the biomass lower heating value, supplied in an ideal combustion process; $\Delta G^0_{\text{cellulose}}$ the cellulose monomer formation Gibbs free energy at standard conditions; and $\Delta H^0_{\text{cellulose}}$ is the cellulose monomer formation enthalpy at standard conditions.

The global exergy efficiency of the plant, obtained with the two methods, is reported in Table 11 for each fuel.

7. Conclusions

The present work demonstrates how the proposed coupling of a recirculated fluidized-bed gasifier and an MCFC system presents high conversion efficiencies (43–49%), which are better than those reached by traditional fossil-fuel plants of the same size.

A significant thermal energy fraction which, if exploited, makes it possible to reach a global exergy efficiency of 78–81%, is released at temperatures of approximately 800 °C on the syngas line (in absence of steam feeding in the gasifier) and 250 °C from the burner exhaust outlet. As the most of the heat is recovered from exhausts at approximately 250 °C, it would be particularly beneficial to exploit it for feeding a district heating plant network. Furthermore, its very low environmental impact make this solution particularly suitable for distributed energy production, especially in small towns situated in mountainous and rural zones where there is often available a large quantity of biomass waste whose disposal costs are usually high. The relocation of the electrical generation would permit a reduction in electrical distribution losses, and would also be able to compete effectively with conventional centralized generation systems.

Acknowledgements

The authors are grateful to Prof. Paolo Costa (DIAM—University of Genoa), Prof. Marco Ragazzi (DICA—University of Trent) and Dr. Filippo Parodi (Ansaldo Fuel Cells S.p.A., Italy) for their generous help during this work.

References

[1] D.O. Hall, R.P. Overend, Biomass, Regenerable Energy, Wiley, Great Britain, 1987.
[2] L. Donald, Klass: Biomass for Renewable Energy, Fuels, and Chemicals, Academic Press, San Diego, CA, 1998.
[3] S. Gordon, B.J. McBride, Computer Program for Calculation of Complex Chemical Equilibrium Composition, Rocket Performance, Incident and Reflected Shocks and Chapman-Jouguet Detonations, NASA Report SP-273, 1971.

[4] W.R. Smith, R.W. Missen, Chemical Reaction Equilibrium Analysis: Theory and Algorithm, Wiley-Interscience, New York, 1982.
[5] California Institute of Technology web page: www.galcit.caltech.edu/EDL/public (June 2005).
[6] D.C. Dayton, Fuel Cell Integration, a Study of the Impacts of Gas Quality And Impurities, National Renewable Energy Laboratory, Golden, CO, 2001.
[7] S.J. Bossart, D.C. Cicero, C.M. Zeh, R.C. Bedick, Gas Stream Clean-Up, Morgantown Energy Technology Center, Morgantown, West Virginia, 1990.
[8] M.C. Williams, Fuel Cell Handbook, fifth ed., U.S. Department of Energy, Morgantown, West Virginia, 2000.
[9] A. Pigeaud, Study of the Effects of Soot, Particulate and Other Contaminants on Molten Carbonate Fuel Cell, Fuelled by Coal Gas, U.S. Department of Energy, Morgantown, West Virginia, 1987.
[10] M. Ronchetti, A. Iacobazzi, Celle a combustibile, stato di sviluppo e prospettive della tecnologia, ENEA, Rome, Italy, 2002.
[11] K.V. Lobachyov, H.J. Richter, Energy Conversion Manage. 39 (1998) 1931–1943.
[12] C. Coppola, B. Bosio, E. Arato, Chem. Eng. Trans. 4 (2004) 277–282, S. Pierucci Editore, AIDIC Servizi S.r.l., Milano.
[13] C. Myrén, C. Hörnell, E. Björnbom, K. Sjöström, Biomass Bioenergy 23 (2002) 217–227.
[14] A. Capria, A.L. De Cesaris, M. Dubini, M. Giugliano, Controllo delle emissioni in atmosfera da impianti industriali, Istituto per l'ambiente, Milan, Italy, 1992.
[15] D. Dellepiane, B. Bosio, E. Arato, J. Power Sources 122 (2003) 47–56.
[16] D. Barabino, D. Dellepiane, B. Bosio, E. Arato, F. Parodi, Chem. Eng. Trans. 3 (2004) 527–532, S. Pierucci Editore, AIDIC Servizi S.r.l., Milano.
[17] B. Bosio, A. Serrafero, E. Arato, Chem. Eng. Trans. 6 (2) (2005) 719–724, S. Pierucci Editore, AIDIC Servizi S.r.l., Milano.
[18] B. Guo, D. Li, C. Cheng, Z.-a. Lü, Y. Shen, Bioresour. Technol. 76 (2001) 77–83.
[19] A. Demirbas, Energy Conversion Manage. 43 (2002) 897–909.
[20] FIRE (Federazione Italiana per l'uso Razionale dell'Energia) internet site: www.fire-italia.it (June 2004).